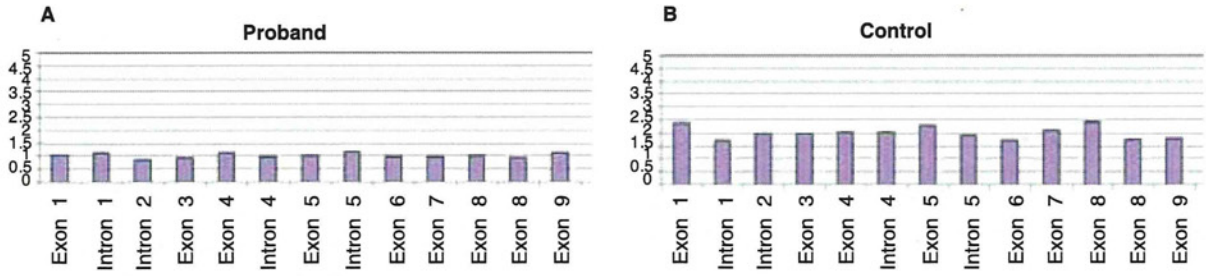

Figure 5. Results of MLPA analysis of *PAX3* in family 2. (A, B) Relative ratios of DNA quantity in each exon compared with that in the control region are shown for the proband (A) and control (B).

missense mutation may be a rare normal variant. Thus, the pathogenicity of such mutations needs to be verified by detection of the same mutation in multiple families with the same phenotype or by functional analysis. The functional consequences of a few *PAX3* mutations have been tested and reduced DNA-binding properties have been reported [13–15]. The p.I59F mutation was reported in a Japanese family [8], but functional analysis has not been conducted. We analyzed the predicted 3D structures of the paired domain of the PAX3-DNA complex and showed that this mutation was likely to distort the structure of the DNA-binding site of PAX3 and lead to functional impairment. This result substantially supports the hypothesis that the p.I59F mutation is pathogenic, although it is based on a theoretical prediction rather than functional experiments.

In family 2, the distinct phenotypes of the proband, the proband's mother, and the proband's grandmother were congenital unilateral hearing loss, heterochromia iridis, and early graying, respectively. Because of these differences, they were not aware of the hereditary nature of the symptoms. Identification of the *PAX3* mutation in the proband and the proband's grandmother led to an accurate diagnosis of WS1 and facilitated understanding of the symptoms. In this family, direct sequencing of *PAX3* did not detect any mutations, but MLPA analysis detected a large heterozygous deletion. Furthermore, quantitative PCR analysis revealed that the deleted region spanned 1759–2554 kb and included 12–18 genes. Large deletions of *PAX3* in patients with WS1 have been reported in several families [6,16–18]. To our knowledge, however, this is the largest deletion identified in patients with WS1 and has, therefore, expanded the spectrum of *PAX3* mutations. There is no reported correlation between the nature of the mutation (deleted vs truncated or missense) or

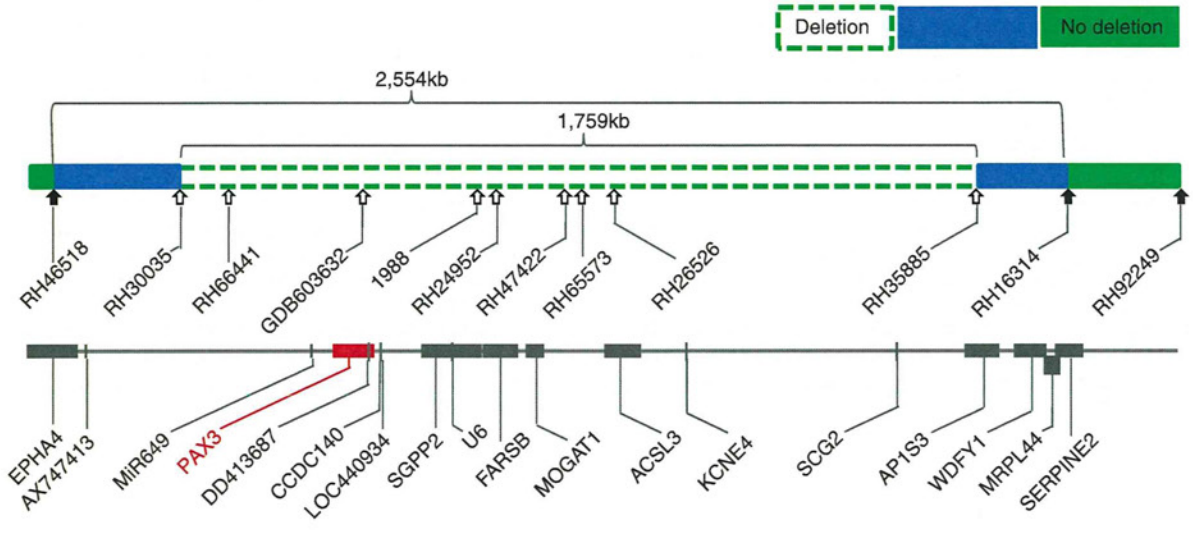

Figure 6. Genetic map showing the estimated location of the *PAX3* deletion together with the regions surrounding *PAX3*. Sites examined by quantitative PCR are indicated by arrows. Blank and white arrows indicate that the quantities of DNA at these sites are half or identical to the quantities of DNA at the corresponding sites in the control, respectively. The 5' and 3' ends of the deletion are located within the blue regions flanking the white region, designated as 'deletion,' and flanked by the green regions, designated as 'no deletion.' All genes mapped within this region, including *PAX3*, are shown in the lower map.

its location in *PAX3*, and the severity of the WS1 phenotype [19,20]. Similarly, no evidence of such a correlation was found in the data presented in this study.

In the present study, *PAX3* genetic diagnosis contributed to the accurate diagnosis of WS1. Such diagnosis could help provide genetic counseling to patients with isolated or few phenotypic symptoms, those with mild phenotypes or few first-degree relatives, or those who have yet to develop any symptoms. In addition, analysis of the predicted 3D structure of PAX3 facilitated the verification of pathogenicity of a missense mutation, and MLPA analysis increased the sensitivity of genetic diagnosis of WS1.

Acknowledgments

We thank the families that participated in this study. This study was supported by a Grant-in-Aid for Clinical Research from the National Hospital Organization, and by a Health and Labour Sciences Research Grants for Research on Rare and Intractable Diseases from the Ministry of Health, Labour and Welfare of Japan.

Declaration of interest: The authors report no conflicts of interest. The authors alone are responsible for the content and writing of the paper.

References

[1] Read AP, Newton VE. Waardenburg syndrome. J Med Genet 1997;34:656–65.

[2] Farrer LA, Grundfast KM, Amos J, Arnos KS, Asher JH Jr, Beighton P, et al. Waardenburg syndrome (WS) type I is caused by defects at multiple loci, one of which is near ALPP on chromosome 2: first report of the WS consortium. Am J Hum Genet 1992;50:902–13.

[3] Liu XZ, Newton VE, Read AP. Waardenburg syndrome type II: phenotypic findings and diagnostic criteria. Am J Med Genet 1995;55:95–100.

[4] Pardono E, van Bever Y, van den Ende J, Havrenne PC, Iughetti P, Maestrelli SR, et al. Waardenburg syndrome: clinical differentiation between types I and II. Am J Med Genet A 2003;117A:223–35.

[5] Pingault V, Ente D, Dastot-Le Moal F, Goossens M, Marlin S, Bondurand N. Review and update of mutations causing Waardenburg syndrome. Hum Mutat 2010;31: 391–406.

[6] Milunsky JM, Maher TA, Ito M, Milunsky A. The value of MLPA in Waardenburg syndrome. Genet Test 2007;11:179–82.

[7] Ishikiriyama S, Tonoki H, Shibuya Y, Chin S, Harada N, Abe K, et al. Waardenburg syndrome type I in a child with de novo inversion (2)(q35q37.3). Am J Med Genet 1989;33: 505–7.

[8] Soejima H, Fujimoto M, Tsukamoto K, Matsumoto N, Yoshiura KI, Fukushima Y, et al. Three novel PAX3 mutations observed in patients with Waardenburg syndrome type 1. Hum Mutat 1997;9:177–80.

[9] Kashima T, Akiyama H, Kishi S. Asymmetric severity of diabetic retinopathy in Waardenburg syndrome. Clin Ophthalmol 2011;5:1717–20.

[10] Kiefer F, Arnold K, Kunzli M, Bordoli L, Schwede T. The SWISS-MODEL Repository and associated resources. Nucleic Acids Res 2009;37:D387–92.

[11] Xu W, Rould MA, Jun S, Desplan C, Pabo CO. Crystal structure of a paired domain-DNA complex at 2. 5 A resolution reveals structural basis for Pax developmental mutations. Cell 1995;80:639–50.

[12] Pettersen EF, Goddard TD, Huang CC, Couch GS, Greenblatt DM, Meng EC, et al. UCSF Chimera – a visualization system for exploratory research and analysis. J Comput Chem 2004;25:1605–12.

[13] Chalepakis G, Goulding M, Read A, Strachan T, Gruss P. Molecular basis of splotch and Waardenburg Pax-3-mutations. Proc Natl Acad Sci USA 1994;91:3685–9.

[14] Corry GN, Underhill DA. Pax3 target gene recognition occurs through distinct modes that are differentially affected by disease-associated mutations. Pigment Cell Res 2005;18: 427–38.

[15] Fortin AS, Underhill DA, Gros P. Reciprocal effect of Waardenburg syndrome mutations on DNA binding by the Pax-3 paired domain and homeodomain. Hum Mol Genet 1997;6:1781–90.

[16] Baldwin CT, Lipsky NR, Hoth CF, Cohen T, Mamuya W, Milunsky A. Mutations in PAX3 associated with Waardenburg syndrome type I. Hum Mutat 1994;3:205–11.

[17] Tassabehji M, Newton VE, Leverton K, Turnbull K, Seemanova E, Kunze J, et al. PAX3 gene structure and mutations: close analogies between Waardenburg syndrome and the Splotch mouse. Hum Mol Genet 1994;3: 1069–74.

[18] Wang J, Li S, Xiao X, Wang P, Guo X, Zhang Q. PAX3 mutations and clinical characteristics in Chinese patients with Waardenburg syndrome type 1. Mol Vis 2010;16:1146–53.

[19] Baldwin CT, Hoth CF, Macina RA, Milunsky A. Mutations in PAX3 that cause Waardenburg syndrome type I: ten new mutations and review of the literature. Am J Med Genet 1995;58:115–22.

[20] Tassabehji M, Newton VE, Liu XZ, Brady A, Donnai D, Krajewska-Walasek M, et al. The mutational spectrum in Waardenburg syndrome. Hum Mol Genet 1995;4: 2131–7.

Acta Oto-Laryngologica, 2012; 132: 1160–1167

informa
healthcare

ORIGINAL ARTICLE

Unilateral cochlear nerve hypoplasia in children with mild to moderate hearing loss

HIDENOBU TAIJI[1], NORIKO MORIMOTO[1] & TATSUO MATSUNAGA[2]

[1]*Department of Otorhinolaryngology, National Center for Child Health and Development and* [2]*Laboratory of Auditory Disorders, National Institute of Sensory Organs, National Tokyo Medical Center, Tokyo, Japan*

Abstract

Conclusion: Even if hearing loss is mild to moderate, the presence of cochlear nerve (CN) hypoplasia associated with retrocochlear disorders should be considered. *Objectives:* CN hypoplasia is a term that refers to an absent cochlear nerve on high-resolution magnetic resonance imaging (MRI). Most cases of CN hypoplasia are associated with profound hearing loss. The present study reports six pediatric cases of unilateral CN hypoplasia with mild to moderate hearing loss. *Methods:* Between May 2008 and April 2011, pure-tone hearing tests were performed in 17 patients who were diagnosed with CN hypoplasia on high resolution for evaluation of unilateral sensorineural hearing loss at the National Center for Child Health and Development. Of these, six patients had average hearing levels in the affected ears of < 60 dB and were therefore included in this study. *Results:* All six ears with CN hypoplasia were associated with CN canal stenosis. DPOAEs were present in one (17%) of the six affected ears. The ABR thresholds of the ears with CN hypoplasia were significantly elevated compared with 1–4 kHz pure-tone hearing levels in one of three cases. In two of five cases, the maximum word recognition scores of the affected ears were poor compared with pure-tone hearing levels.

Keywords: *3-D constructive interference, steady-state magnetic resonance imaging, word recognition score, sensorineural hearing loss*

Introduction

Cochlear nerve (CN) hypoplasia refers to the absence of a visible CN on oblique sagittal magnetic resonance (MR) images of the lateral aspect of the inner auditory canal (IAC). CN hypoplasia is not an uncommon cause of congenital hearing loss as previously thought [1,2]. Although it is believed that most cases of CN hypoplasia are associated with profound hearing loss [1], a recent report presented a case of CN hypoplasia with moderate hearing loss limited to high frequencies [3]. The present study reports six pediatric cases of unilateral CN hypoplasia with mild to moderate hearing loss, and demonstrates that retrocochlear hearing loss is the predominant audiologic characteristic in these children.

Material and methods

Patient population

Between May 2008 and April 2011, 25 children who presented for evaluation of unilateral sensorineural hearing loss (SNHL) at the National Center for Child Health and Development were diagnosed with CN hypoplasia on high-resolution MR imaging (MRI).

Pure-tone hearing tests could be performed in 17 of these 25 children. Pure-tone audiometry was evaluated based on the three-tone average formulated by (a+b+c)/3, where a, b, and c are hearing levels at 0.5, 1, and 2 kHz, respectively. Eleven cases had profound hearing loss in the affected ears, with average hearing levels of >90 dB. The average hearing levels

Correspondence: Hidenobu Taiji MD, Department of Otorhinolaryngology, National Center for Child Health and Development, 2-10-1 Okura, Setagaya-ku, Tokyo 157-8535, Japan. Tel: +81 3 3416 0181. Fax: +81 3 5494 7909. E-mail: taijih5@gmail.com

(Received 20 April 2012; accepted 12 May 2012)

ISSN 0001-6489 print/ISSN 1651-2251 online
DOI: 10.3109/00016489.2012.696781

Table I. Audiologic and radiologic findings in children with unilateral cochlear nerve (CN) hypoplasia.

			Audiologic findings in affected ear				CNC diameter (mm)	
Case no.	Age (years)/sex	Side	Pure-tone hearing level (dB)	ABR thresholds (dB nHL)	Maximum speech discrimination (%)	DPOAE	Affected ear	Healthy ear
1	6/F	R	41	80	25	Absent	1.2	1.7
2	5/F	L	35	90	60	Absent	0.7	1.9
3	8/F	R	59	–	70	Absent	0.5	1.7
4	8/M	R	38	–	90	Normal	1.3	2.0
5	13/F	L	59	–	50	Absent	1.0	2.1
6	4/F	R	40	60	–	Absent	0.3	1.8

–, not evaluated; ABR, auditory brainstem response; CNC, cochlear nerve canal; DPOAE, distortion product otoacoustic emission; F, female; M, male.

of the affected ears in the remaining six (24%) cases were <60 dB (Table I). These six patients were therefore included in this study for further analysis.

The six pediatric cases consisted of one boy and five girls with a mean age of 7.3 years (range, 4–13 years). None of the children had known syndromes that could cause hearing loss or risk factors of hearing loss such as a history of prematurity, hypoxia, and hyperbilirubinemia.

Imaging

High-resolution computed tomography (HRCT) of the temporal bone in all patients was performed with

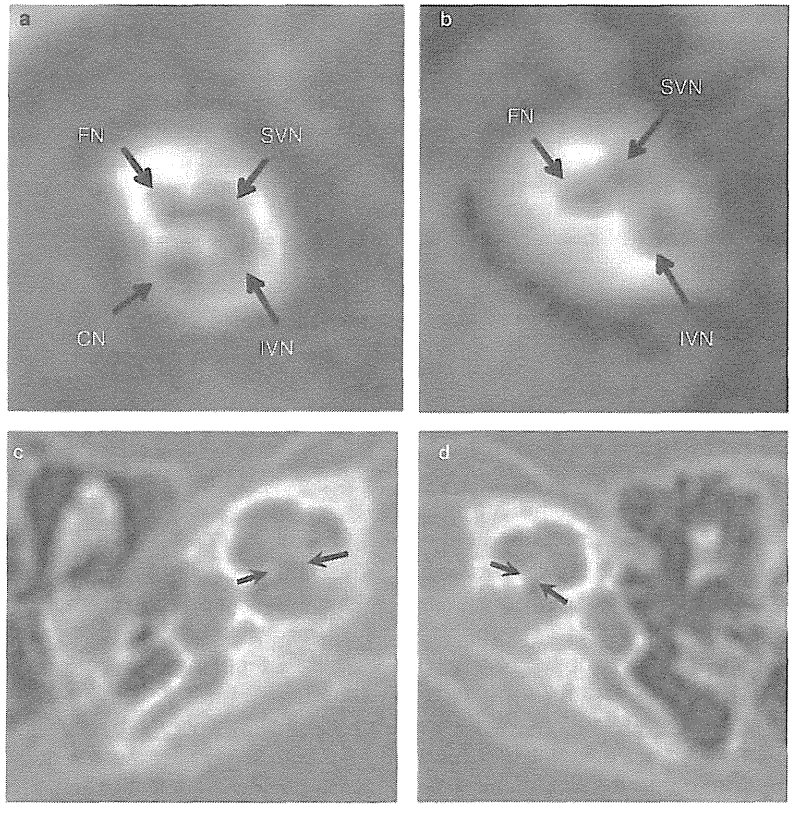

Figure 1. Cochlear nerve hypoplasia in a 5-year-old girl with left sensorineural hearing loss (SNHL) (case 2). (a, b) Oblique sagittal magnetic resonance (MR) images of the inner auditory canal (IAC). Four nerves were detected in the right (a), while the left cochlear nerve is not visible (b). CN, cochlear nerve; FN, facial nerve; IVN, inferior vestibular nerve; SVN, superior vestibular nerve. (c, d) Axial images of temporal bone high-resolution computed tomography (HRCT) show narrowing of left cochlear nerve canal (CNC) (d, 0.7 mm) compared with the right CNC (c, 1.9 mm).

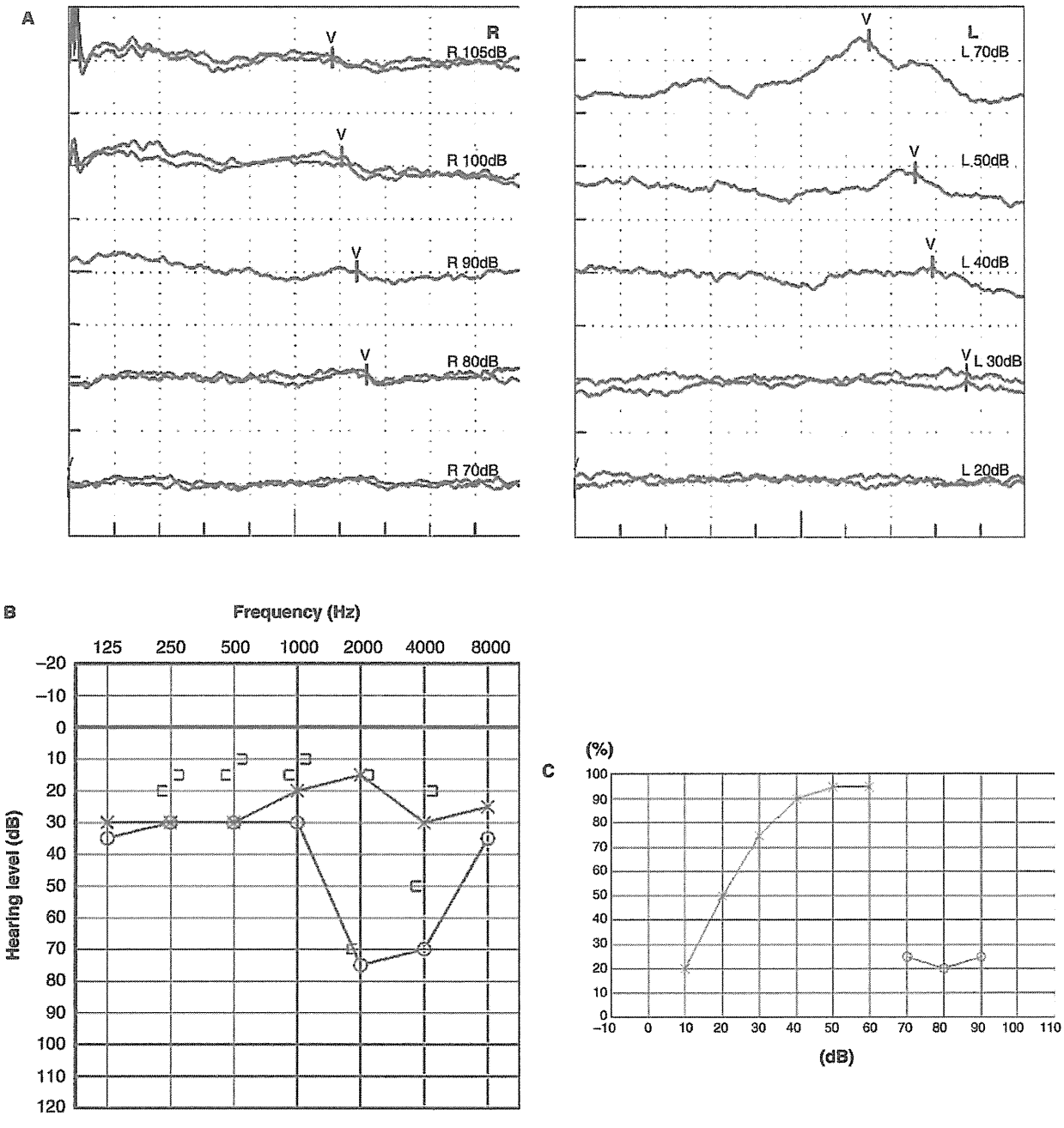

Figure 2. Audiologic findings in a child with right-sided cochlear nerve hypoplasia (case 1). (A) Auditory brainstem responses (ABRs), (B) pure-tone audiogram, (C) word recognition curve.

a multidetector-row CT scanner (8-detector, Lightspeed Ultra, GE, Milwaukee, USA). Images were acquired in the direct axial planes using a 0.652 mm slice thickness. The diameter of the CN canal (CNC) was measured along the inner margin of its bony walls at its middle portion on the axial image of the base of the modiolus.

MR images were obtained using a 1.5 Tesla system (Intera 1.5T; Philips, Belgium) according to a protocol described previously in detail [4]. The MRI scans included 3-D T2-weighted fast spin-echo sequences in axial and oblique sagittal images of the IAC with a 0.7 mm slice thickness. The 3-D constructive interference in steady-state (CISS) images was then reconstructed by traversing the IAC in a perpendicular orientation, producing images that visualized the four nerves (facial, superior vestibular, inferior vestibular, and cochlear). The

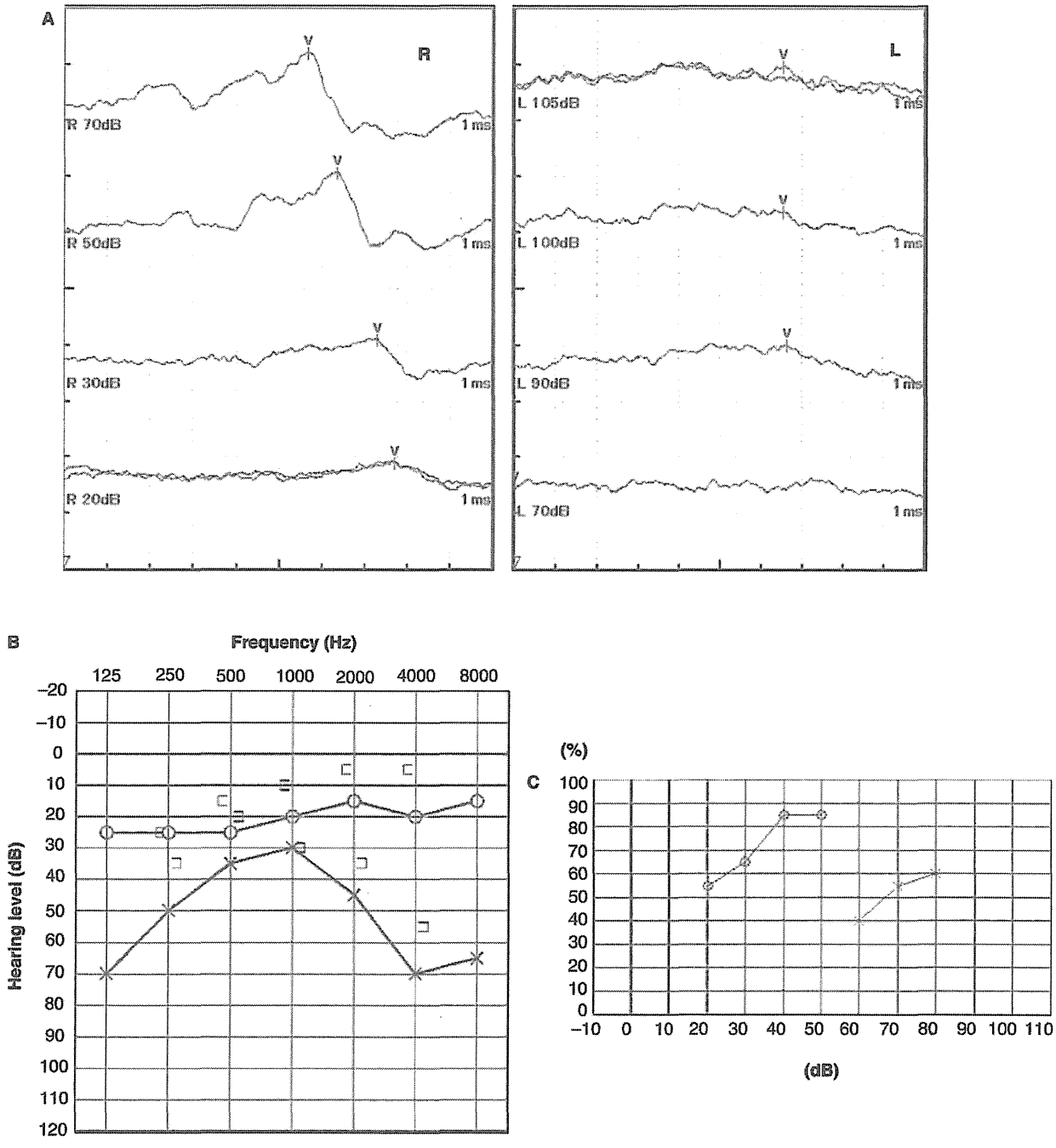

Figure 3. Audiologic findings in a child with left-sided cochlear nerve hypoplasia (case 2). (A) Auditory brainstem responses (ABRs), (B) pure-tone audiogram, (C) word recognition curve.

findings of a normal ear are shown in Figure 1a, b, (case 2, right ear).

Audiologic assessment

In addition to the pure-tone hearing test, distortion product otoacoustic emission (DPOAE) and auditory brainstem response (ABR) testing, as well as speech audiometry were performed. DPOAEs were measured in all subjects for pairs of primary tones (f1 and f2), with a fixed ratio of f2/f1 = 1.2, and fixed levels of 65 dB SPL (L1) and 55 dB SPL (L2) using the ILO292 system (Otodynamics, UK). The frequency of f2 was stepped through a range of 1–6 kHz to yield a nine-point DPGram.

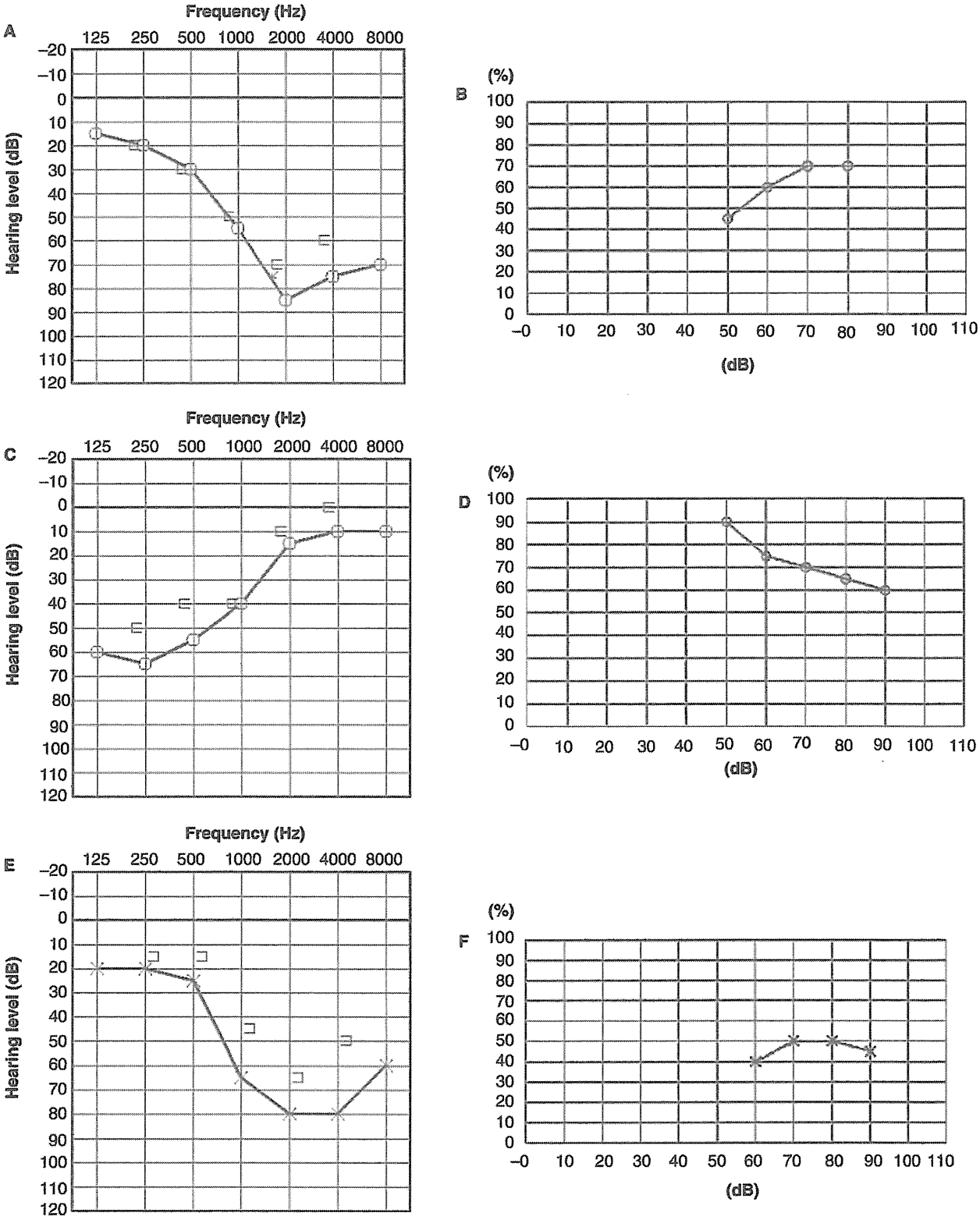

Figure 4. Audiologic findings in ears with cochlear nerve hypoplasia (cases 3–5). (a, c, e) Pure-tone audiograms: (a) case 3, (c) case 4, (e) case 5. (b, d, f) Word recognition curves: (b) case 3, (d) case 4, (f) case 5.

ABRs were recorded in three subjects using the MEB-2204 system (Nihon Koden, Japan). The 0.1 ms clicks with alternating polarity were presented monaurally at a repetition rate of 10 Hz and a maximum intensity of 105 dB nHL.

Speech audiometry was performed in five subjects, but not in case 6 where the test could not be done. The maximum word recognition scores were evaluated based on the percentage of correct answers out of 20 words, using Japanese word list 67-S. In normal-hearing subjects, the maximum word recognition scores using the word list are usually ≥90%.

Results

A summary of the findings for the six children with unilateral CN hypoplasia diagnosed by MRI is shown in Table I. On the oblique sagittal MRI image of case 2, the left CN is undetectable, while the right CN is normal (Figure 1a, b). The hearing levels of the affected ears in the six cases ranged from 35 to 59 dB (Table I). The audiogram shapes (Figures 2, 3, and 4) were high-frequency sloping (cases 3, 5, and 6), rising (case 4), 2–4 kHz notch (case 1), and inverted scoop shape (case 2). DPOAEs were present in only one (17%) of the six affected ears, and the shape of the hearing loss curve for that ear was rising.

In one of the three cases in which ABR testing was performed, the ABR threshold of the ear with CN hypoplasia was significantly elevated compared with that expected from 1000–4000 Hz pure-tone hearing levels (case 2). Speech discrimination tests were performed in five cases (Figures 2c, 3c, and 4b, d, f) but not in the 4-year-old patient (case 6). In two of these five cases (cases 1 and 2), the maximum word recognition scores of the ears with CN hypoplasia were poor compared with those of pure-tone hearing levels. In one case (case 4), the maximum word recognition score of the affected ear was 90%, but the results for 50 dB and 90 dB were 90% and 60%, respectively. Therefore, the word recognition curve in case 4 showed marked roll-over.

The click-evoked ABR tracing, pure-tone audiogram, and word recognition curves for case 1 are shown in Figure 2. The pure-tone audiogram of the right ear (affected side) showed a 2–4 kHz notch configuration. The wave V threshold of the right ear was elevated (80 dB nHL). The ABR threshold compared with the 1–4 kHz pure-tone hearing level of the right ear was slightly higher than expected. The maximum word recognition score of the right ear was 25%, which was lower than expected for pure-tone hearing.

The click-evoked ABR tracing, pure-tone audiogram, and word recognition curves for case 2 are shown in Figure 3. The pure-tone audiogram of the left ear (affected side) showed an inverted scoop shape. The ABR threshold of the left ear was 90 dB nHL and the maximum word recognition score of the left ear was 60%. These values were smaller than expected for pure-tone hearing.

All six ears with CN hypoplasia were associated with CNC stenosis (CNC diameter, <1.5 mm; mean, 0.83 mm). In contrast, the unaffected ears of the six children had CNC diameters of >1.5 mm (mean, 1.9 mm). Axial HRCT images of a representative case (case 2) of severe CNC stenosis are shown in Figure 1c and d. No cochlear malformations were seen in the six children.

Discussion

We defined CN hypoplasia as an undetectable CN on axial, coronal, or reconstructed oblique sagittal MR images. An extremely small nerve, below the limits of resolution of MRI, could appear absent and therefore should not be disregarded. Therefore, we avoid the terms deficiency, aplasia, and agenesis.

The mechanism of CN hypoplasia in children remains speculative. Both congenital deficiency and acquired degeneration of the CN might be seen in children with SNHL [5]. In pediatric cases, it is possible that a vascular insult during critical periods in development may result in isolated CN agenesis or degeneration [1]. CN hypoplasia is often associated with cochlear anomalies [4] or various coexisting syndromes such as CHARGE association [1]. Neither cochlear malformations nor known syndromes were recognized in the patients presented in this report.

CN hypoplasia is not as uncommon as previously thought [1]. Recent studies suggest that CN dysfunction accounts for up to 10% of diagnosed cases of pediatric SNHL [2]. Miyasaka et al. [4] reported CN hypoplasia in 8 of 42 (19%) ears on MRI. Of these, four ears had inner ear malformations. In the present study, no cochlear malformations were recognized in the six ears with CN hypoplasia. In addition, a relationship between CNC stenosis and CN hypoplasia was previously reported [2,6,7]. CNC diameter measurements of <1.8 mm were considered moderate stenosis, while measurements of <1.0 mm were defined as critical stenosis [8]. A CNC diameter of <1.5 mm on CT suggested CN hypoplasia [4,6,7]. All six ears with CN hypoplasia in this study were associated with CNC stenosis (CNC diameter, <1.5 mm). And also 11 ears with CN hypoplasia with profound hearing loss were associated with CNC stenosis. The mean (SD) CNC diameter was 0.83 (0.40) mm in the affected side of 6 cases with mild to moderate hearing loss, and 0.72 (0.32) mm in the affected side of 11 cases with profound hearing

loss. The CNC diameters in the group with profound hearing loss were slightly narrower than in the group with mild to moderate hearing loss, but there was no statistically significant difference ($p = 0.28$, t test). CNC may require stimulation by its contents for normal development, meaning that CNC stenosis may occur secondary to CN hypoplasia [6]. However, it was previously reported that CNC stenosis can occur without CN hypoplasia [4]. CNC stenosis on CT may therefore be indicative of the diagnosis of CN hypoplasia, but MRI should be performed to confirm the diagnosis.

In the past, it was thought that CN hypoplasia was always associated with profound SNHL [1], but a case of CN hypoplasia without profound hearing loss was reported recently [3]. In that case, an extremely small, preserved, and partially functional CN was believed to be present in the affected ear [3]. A minimal number of residual CN fibers, which were too small to be detected by MRI, may be enough to deliver sound information without threshold elevation [8].

CN hypoplasia may present as auditory neuropathy spectrum disorder (ANSD) [1,9]. In this study, DPOAEs were detected in one of six cases, which indicated normal outer hair cell function. In the 11 cases of CN hypoplasia with profound hearing loss, DPOAEs at the affected ears were detected in four cases (36%). The presence rates of DPOAEs were supposed not to relate to hearing levels. The reason for absent DPOAEs in cases of mild hearing loss is unclear, but malformations of inner ear microstructures associated with congenital CN hypoplasia are considered to be the cause of absent DPOAEs. The shape of the hearing loss curve in the case with normal DPOAE was rising (Figure 4c), and the pure-tone thresholds at 2–8 kHz were ≤15 dB. The normal DPOAE response in this case is assumed to indicate the preservation of inner ear function at high frequencies.

In case 2, who was one of three cases in which ABR testing was performed, the ABR threshold of the affected ear was significantly elevated compared with that expected from 1–4 kHz pure-tone hearing levels. The elevated ABR threshold in the case suggests disorders of CN synchrony at high frequencies.

Speech discrimination assessments showed poor maximum word recognition scores compared with that expected from pure-tone hearing levels in two affected ears. In addition, the word recognition curve of an affected ear had marked roll-over. The results of the speech discrimination tests suggested retrocochlear disorders in the affected ears. Some of the findings of the ABR and the word recognition tests in CN hypoplasia are consistent with audiologic characteristics of ANSD, which has been reported as retrocochlear hearing loss in CN hypoplasia [1]. It is believed that 6–28% of ANSD cases are due to CN hypoplasia [1,10,11]. CT is recommended for the initial screening of children with SNHL [4]. For children with ANSD, high-resolution MRI of the CN should be performed as the initial imaging study [12]. The results of the present study suggest that the imaging study for the screening of CN hypoplasia is desirable for even mild to moderate hearing loss.

Conclusion

Here, we presented six pediatric cases of CN hypoplasia with mild to moderate hearing loss. Audiologic characteristics of some ears with CN hypoplasia in this study suggested retrocochlear disorders. Even if hearing loss is mild to moderate, the presence of CN hypoplasia associated with retrocochlear disorders should be considered.

Declaration of interest: The authors report no conflicts of interest. The authors alone are responsible for the content and writing of the paper.

References

[1] Buchman CA, Roush PA, Teagle FB, Brown CJ, Zdanski CJ, Grose JH. Auditory neuropathy characteristics in children with cochlear nerve deficiency. Ear Hear 2006; 27:399–408.

[2] Adunka OF, Roush PA, Teagle HF, Brown CJ, Zdanski CJ, Jewells V, et al. Internal auditory canal morphology in children with cochlear nerve deficiency. Otol Neurotol 2006;27: 793–801.

[3] Miyanohara I, Miyashita K, Takumi K, Nakajo M, Kurono Y. A case of cochlear nerve deficiency without profound sensorineural hearing loss. Otol Neurotol 2011; 32:529–32.

[4] Miyasaka M, Nosaka S, Morimoto N, Taiji H, Masaki H. CT and MR imaging for pediatric cochlear implantation: emphasis on the relationship between the cochlear nerve canal and the cochlear nerve. Pediatr Radiol 2010;40: 1509–16.

[5] Glastonbury CM, Davidson HC, Harnsberger HR, Butker J, Kertesz TR, Shelton C. Imaging findings of cochlear nerve deficiency. AJNR 2002;23:635–43.

[6] Kono T. Computed tomographic features of the bony canal of the cochlear nerve in pediatric patients with unilateral sensorineural hearing loss. Radiat Med 2008;26:115–19.

[7] Komatsubara S, Haruta A, Nagano Y, Kodama T. Evaluation of cochlear nerve imaging in severe congenital sensorineural hearing loss. ORL J Otorhinolaryngol Relat Spec 2007;69:198–202.

[8] Valero J, Blaser S, Papsin BC, James AL, Gordon KA. Electrophysiologic and behavioral outcomes of cochlear implantation in children with auditory nerve hypoplasia. Ear Hear 2012;33:3–18.

[9] O'Leary SJ, Gibson WP. Surviving cochlear function in the presence of auditory nerve agenesis. J Laryngol Otol 1999; 113:1008–10.

[10] Walton J, Gibson WP, Sanli H, Prelog K. Predicting cochlear implant outcomes in children with auditory neuropathy. Otol Neurotol 2008;29:302–9.

[11] Teagle HF, Roush PA, Woodard JS, Hatch DR, Zdanski CJ, Buss E, et al. Cochlear implantation in children with auditory neuropathy spectrum disorder. Ear Hear 2010;31:325–35.

[12] Roche JP, Huang BY, Castillo M, Bassim MK, Adunka OF, Buchman CA. Imaging characteristics of children with auditory neuropathy spectrum disorder. Otol Neurotol 2010;31:780–8.

CLINICAL GENETICS An International Journal of Genetics, Molecular and Personalized Medicine

Clin Genet 2012: 82: 425–432
Printed in Singapore. All rights reserved

CLINICAL GENETICS
doi: 10.1111/j.1399-0004.2012.01897.x

Original Article

A prevalent founder mutation and genotype–phenotype correlations of *OTOF* in Japanese patients with auditory neuropathy

Matsunaga T, Mutai H, Kunishima S, Namba K, Morimoto N, Shinjo Y, Arimoto Y, Kataoka Y, Shintani T, Morita N, Sugiuchi T, Masuda S, Nakano A, Taiji H, Kaga K. A prevalent founder mutation and genotype–phenotype correlations of *OTOF* in Japanese patients with auditory neuropathy.
Clin Genet 2012: 82: 425–432. © John Wiley & Sons A/S, 2012

Auditory neuropathy is a hearing disorder characterized by normal outer hair cell function and abnormal neural conduction of the auditory pathway. Aetiology and clinical presentation of congenital or early-onset auditory neuropathy are heterogeneous, and their correlations are not well understood. Genetic backgrounds and associated phenotypes of congenital or early-onset auditory neuropathy were investigated by systematically screening a cohort of 23 patients from unrelated Japanese families. Of the 23 patients, 13 (56.5%) had biallelic mutations in *OTOF*, whereas little or no association was detected with *GJB2* or *PJVK*, respectively. Nine different mutations of *OTOF* were detected, and seven of them were novel. p.R1939Q, which was previously reported in one family in the United States, was found in 13 of the 23 patients (56.5%), and a founder effect was determined for this mutation. p.R1939Q homozygotes and compound heterozygotes of p.R1939Q and truncating mutations or a putative splice site mutation presented with stable, and severe-to-profound hearing loss with a flat or gently sloping audiogram, whereas patients who had non-truncating mutations except for p.R1939Q presented with moderate hearing loss with a steeply sloping, gently sloping or flat audiogram, or temperature-sensitive auditory neuropathy. These results support the clinical significance of comprehensive mutation screening for auditory neuropathy.

Conflict of interest

The authors declare no conflict of interest.

T Matsunaga[a], H Mutai[a], S Kunishima[b], K Namba[a], N Morimoto[c], Y Shinjo[d], Y Arimoto[e], Y Kataoka[f], T Shintani[g], N Morita[h], T Sugiuchi[i], S Masuda[j], A Nakano[e], H Taiji[c] and K Kaga[d]

[a]Laboratory of Auditory Disorders, National Institute of Sensory Organs, National Tokyo Medical Center, Tokyo, Japan, [b]Department of Advanced Diagnosis, Clinical Research Center, National Hospital Organization Nagoya Medical Center, Nagoya, Japan, [c]Department of Otorhinolaryngology, National Center for Child Health and Development, Tokyo, Japan, [d]National Institute of Sensory Organs, National Hospital Organization Tokyo Medical Center, Tokyo, Japan, [e]Division of Otorhinolaryngology, Chiba Children's Hospital, Chiba, Japan, [f]Department of Otolaryngology, Head and Neck Surgery, Okayama University Postgraduate School of Medicine, Dentistry and Pharmaceutical Science, Okayama, Japan, [g]Department of Otolaryngology, Sapporo Medical University School of Medicine, Sapporo, Japan, [h]Department of Otolaryngology, Teikyo University School of Medicine, Tokyo, Japan, [i]Department of Otolaryngology, Kanto Rosai Hospital, Kawasaki, Japan, and [j]Department of Otorhinolaryngology, Institute for Clinical Research, National Mie Hospital, Tsu, Japan

Key words: auditory neuropathy – genotype–phenotype correlation – mutation – non-syndromic hearing loss – *OTOF*

Corresponding author: Tatsuo Matsunaga MD, PhD, Laboratory of Auditory Disorders and Department of Otolaryngology, National Institute of Sensory Organs, National Tokyo Medical Center, 2-5-1 Higashigaoka, Meguro, Tokyo 152-8902, Japan.

Tel.: +81 3 3411 0111;
fax: +81 3 3412 9811;
e-mail:
matsunagatatsuo@kankakuki.go.jp

Received 28 February 2012, revised and accepted for publication 6 April 2012

Auditory neuropathy (AN) is a hearing disorder characterized by normal outer hair cell function, as revealed by the presence of otoacoustic emissions (OAE) or cochlear microphonics, and abnormal neural conduction of the auditory pathway, as revealed by the absence or severe abnormality of auditory brainstem responses (ABR) (1). Hearing disorders having the same characteristics have also been reported as auditory nerve disease in adult cases (2). Individuals with AN invariably have difficulties in understanding speech (3), and approximately 10% of infants diagnosed with profound hearing loss have AN (3, 4).

About 50% of subjects with congenital or early-onset AN have risk factors such as perinatal hypoxia, whereas the remaining 50% of subjects are likely to have a genetic factor (3, 5). To date, four loci responsible for non-syndromic AN have been mapped: DFNB9 caused by *OTOF* mutation and DFNB59 caused by *PJVK* mutation, both of which are responsible for autosomal recessive AN; AUNA1 caused by DIAPH3 mutation, which is responsible for autosomal dominant AN; and AUNX1, which is responsible for X-linked AN (6–9). Mutations in *OTOF*, which contains 50 exons and encodes short and long isoforms of otoferlin (10), are the most frequent mutations associated with AN with various frequency depending on the population studied (11–15). Most *OTOF* genotypes have been associated with stable, severe-to-profound hearing loss with only a few exceptions (11–20). Studies of genetic backgrounds and clinical phenotypes in various populations will extend our knowledge of genotype–phenotype correlations and may help in the management and treatment of AN.

Materials and methods

Subjects

We enrolled 23 index patients of unrelated Japanese families with congenital or early-onset AN. Diagnosis of hearing loss was made by age 2 in all patients except for one, who had mild hearing loss diagnosed at age 9. All patients had non-syndromic AN in both ears, and they were collected from all over Japan as part of a multicentre study of AN. Patients with hearing loss of possible environmental risk factors for AN such as neonatal hypoxia or jaundice were excluded. With regard to the family history, one patient had a brother having congenital AN and all others were simplex. DNA samples and medical information were obtained from each proband and, if possible, parents and siblings. For DNA samples, 2 parents, 1 parent, no parent, and 1 sibling were available in 10 families, 4 families, 9 families, and 1 family, respectively. None of parents of 23 index patients complained of hearing loss by clinical interview. For the normal-hearing control, 189 subjects who had normal hearing by pure-tone audiometry were used. This study was approved by the institutional ethics review board at the National Tokyo Medical Center. Written informed consent was obtained from all the subjects included in the study or their parents.

Genetic analysis

DNA was extracted from peripheral blood by standard procedures. Genetic analysis for mutations in *GJB2* and for A1555G and A3243G mitochondrial DNA mutations were conducted in all patients according to published methods (21, 22). Mutation screening of *OTOF* was performed by bidirectional sequencing of amplicons generated by PCR amplification of each exon (exons 1–50) and splice sites using an ABI 3730 Genetic Analyzer (Applied Biosystems, Foster City, CA). Primer sequences for *OTOF* are listed in Table S1, supporting information. Mutation nomenclature is based on genomic DNA sequence (GenBank accession number NG_009937.1), with the A of the translation initiation codon considered as +1. The nucleotide conservation between mammalian species was evaluated by ClustalW (http://www.ebi.ac.uk/Tools/msa/clustalw2/).

To determine whether the prevalent p.R1939Q alleles are derived from a common founder, we conducted haplotype analysis. We genotyped single nucleotide polymorphisms (SNPs) with a minor allele frequency of >0.3 in the Japanese population and a microsatellite marker (D2S2350) spanning the *OTOF* locus and nearby genes on an ABI Genetic Analyzer 310 and Genescan 3.7 software (Applied Biosystems). Forty-four SNPs and the D2S2350 microsatellite marker in the vicinity of the mutation were genotyped in 11 AN patients who had p.R1939Q and in a part of their parents.

In six patients who did not have any mutations in *OTOF* and *GJB2* and three patients who were heterozygous for *OTOF* mutation without any mutations in *GJB2*, all coding exons and splice sites of *PJVK* were sequenced. Primer sequences were designed based on the reference sequence of *PJVK* (GenBank accession number NG_012186) and are listed in Table S2. Novelty of mutations and non-pathogenic variants found in the present study were examined in EVS (http://evs.gs.washington.edu/EVS/) and dbSNP

(http://www.ncbi.nlm.nih.gov/snp). The effect of an amino acid substitution was predicted using PolyPhen-2 software (http://genetics.bwh.harvard.edu/pph2/) and NNSPLICE 0.9 version (Berkley Drosophila Genome Project, http://www.fruitfly.org/seq_tools/splice.html) for the splice sites. The effect of p.D1842N was also analysed by modelling the three-dimensional structure of otoferlin using SWISS-MODEL (http://swissmodel.expasy.org/) (23).

Clinical examination and data analysis

Audiological tests included otoscopic examination and pure-tone audiometry with a diagnostic audiometer in a soundproof room following International Standards Organization standards. On the basis of pure-tone air-conduction thresholds, the degree of hearing loss was determined by the better ear pure-tone average across the frequencies 0.5, 1, 2, and 4 kHz, and it was classified as mild (20–40 dB), moderate (41–70 dB), severe (71–95 dB), or profound (>95 dB) according to the recommendations for the description of audiological data by the Hereditary Hearing Loss Homepage (http://hereditaryhearingloss.org).

Results

Genetic findings

Of 23 patients with a diagnosis of congenital or early-onset AN, 13 (56.5%) carried two pathogenic *OTOF* alleles, and 3 patients (13.0%) carried one pathogenic allele (Fig. 1: inner circle). In summary, 70% of the patients had pathogenic *OTOF* alleles. Results of genotyping of the detected pathogenic *OTOF* alleles in 13 families carrying two pathogenic *OTOF* alleles (10 families in which two parents were examined and 3 families in which one parent was examined) were compatible with autosomal recessive inheritance in all these families. *OTOF* mutations consisted of three missense mutations, one frameshift mutation, two nonsense mutations, one non-stop mutation, and two putative splice site mutations (Tables 1 and 2). p.R1939Q was previously reported as a mutation and IVS47-2A>G was previously reported in dbSNP. Other seven *OTOF* mutations were novel. p.R1939Q was found in 43.5% of all alleles. We also identified 16 non-pathogenic *OTOF* variants, of which only p.P1697P was novel (Table 1). This variant did not change the score of splice site prediction. The location of each mutation in *OTOF* and the evolutionary conservation of the amino acids or nucleotides affected by the missense and putative splice site mutations are shown in Fig. 2a,b. The frequency of different *OTOF* genotypes is summarized in Fig. 1 (middle circle); 56.5% of the patients had p.R1939Q. In contrast, mutations other than p.R1939Q were confined to individual families. Previously, p.R1939Q was reported in one family with AN in the United States (19), and a different mutation in the same codon (p.R1939W) was reported in another family (16). Screening for the mutation

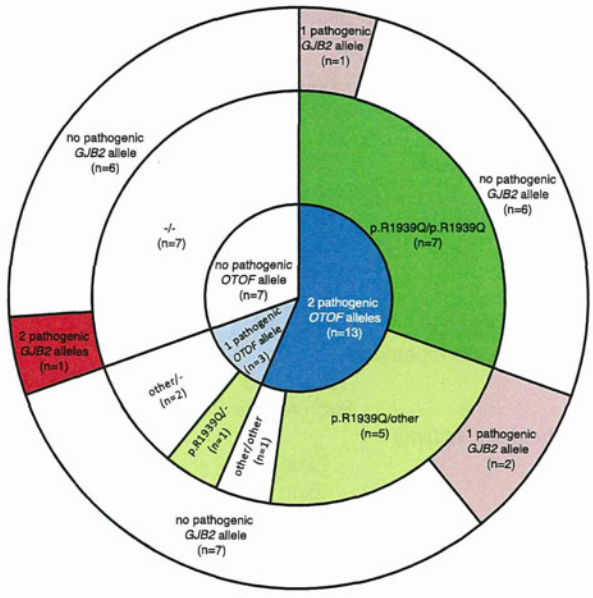

Fig. 1. Genetic backgrounds and frequency of different *OTOF* alleles in patients with congenital or early-onset auditory neuropathy (AN). (a) Distribution of patients carrying different pathogenic *OTOF* alleles (inner circle), *OTOF* genotypes (middle circle), and *GJB2* genotypes (outer circle). p.R1939Q indicates *OTOF* allele with p.R1939Q mutation; other indicates pathogenic *OTOF* alleles except for p.R1939Q allele; *n* indicates number of patients.

in 189 control subjects with normal hearing revealed only one heterozygous carrier. This mutation was predicted to be probably damaging variant according to PolyPhen-2.

The novel missense mutation p.D1842N was identified in a heterozygote without accompanying pathogenic alleles (patient 15). The mutation was predicted to be probably damaging variant according to PolyPhen-2. D1842 is located within the C2F domain, which is one of six calcium-binding modules (C2 domains) in otoferlin that are indispensable for otoferlin function. The predicted three-dimensional protein structure suggested that this mutation generates a repulsive force on calcium ions, resulting in reduced otoferlin activity (Fig. 3a–c). Another novel missense mutation, p.G541S, was identified as homozygous in a patient with parental consanguinity (patient 13). This mutation was predicted to be probably damaging variant according to PolyPhen-2 and involves a change from a non-polar residue to a polar residue in the C2C domain.

The c.1946-1965 del20 frameshift mutation truncates otoferlin at S648, causing a change in stop codon that adds six residues to the C terminus. Two nonsense mutations, p.Y474X and p.Y1822X, also truncate otoferlin. It is possible that these mutations trigger the nonsense-mediated decay response, by which aberrant mRNA is eliminated before translation (24). Even if the truncated proteins were produced, they would not function well because the mutations in c.1946-1965 del20, p.Y474X, and p.Y1822X disrupt three

Table 1. Mutations and non-pathogenic variants in congenital or early-onset auditory neuropathy

Types of variants	Location	Nucleotide variation	Predicted amino acid change	Allele frequency in normal controls	Novel or known
Mutations					
Missense substitution	Exon 15	c.1621G>A	p.G541S	0/376	Novel
	Exon 46	c.5524G>A	p.D1842N	0/376	Novel
	Exon 50	c.5816G>A	p.R1939Q	1/378	Known
Frameshift	Exon 17	c.1946-1965del20	p.R649PfsX5	0/192	Novel
Nonsense	Exon 14	c.1422T>A	p.Y474X	0/192	Novel
	Exon 46	c.5466C>G	p.Y1822X	0/192	Novel
Non-stop substitution	Exon 50	c.5992T>C	p.X1988RextX30	0/192	Novel
Putative splice site mutations					
	Exon 9 IVS	IVS9+5G>A		0/362	Novel
	Exon 47 IVS	IVS47-2A>G		0/190	Known
Non-pathogenic variants					
	Exon 2	c.129C>T	p.D43D	NT	Known
	Exon 3	c.145C>T	p.R49W	3/192	Known
	Exon 3	c.158C>T	p.A53V	75/192	Known
	Exon 4	c.244C>T	p.R82C	29/192	Known
	Exon 5	c.372A>G	p.T124T	NT	Known
	Exon 19	c.62C>T	p.P21L	172/172	Known
	Exon 23	c.2452C>T	p.R818W	0/188	Known
	Exon 24	c.2580C>G	p.V860V	NT	Known
	Exon 24	c.2613C>T	p.L861L	NT	Known
	Exon 25	c.2703G>A	p.S901S	NT	Known
	Exon 25	c.2736G>C	p.L912L	NT	Known
	Exon 41	c.4677G>A	p.V1559V	NT	Known
	Exon 41	c.4767C>T	p.R1589R	NT	Known
	Exon 43	c.5026C>T	p.R1676C	8/188	Known
	Exon 43	c.5091G>A	p.P1697P	NT	Novel
	Exon 45	c.5331C>T	p.D1777D	NT	Known

C2 domains, four C2 domains, and one C2 domain, respectively.

p.X1988RextX30, in which the stop codon is affected and 30 residues are added to the C terminus, accompanied p.R1939Q in a compound heterozygote (patient 12). Because the stop codon is separated by only one residue from the transmembrane domain, the additional C-terminal tail residues would interfere with anchoring to the membrane, which is critical for proper function. The three subjects with only one pathogenic *OTOF* allele (patient 14, patient 15, and patient 16) are likely to have mutations which could not be identified in the present study rather than just be coincidental carriers. Mutations which were not excluded in the present study include those in introns, a previously unknown exon, or a distant enhancer/promotor region as well as large deletions or other sequence rearrangements.

Screening of other genes revealed that one patient who did not have any mutations in *OTOF* was a compound heterozygote of *GJB2* mutations (patient 21). The AN phenotype has been reported in subjects with *GJB2* mutations (25). We identified three other patients with biallelic *OTOF* mutations that had heterozygous *GJB2* mutations, but they were considered to be coincidental. Distribution of patients carrying different pathogenic GJB2 alleles was shown in Fig. 1 (outer circle). None of the patients had A1555G or A3243G mitochondrial DNA mutations. Mutations in *PJVK* were not detected in six patients who did not have any mutations in *OTOF* or *GJB2* as well as in three patients who were heterozygous for *OTOF* mutation without mutations in *GJB2*.

All but one patient had a single haplotype associated with the p.R1939Q variant, which was not represented in 22 wild-type alleles in the parents, and representative SNPs and their allele frequencies as well as haplotypes are shown in Fig. 4a,b. Patient 2 had recombination of the same p.R1939Q-associated haplotype with the wild-type haplotype from his father. These results indicated that all the chromosomes carrying p.R1939Q were derived from a common ancestor.

Clinical findings

Clinical features of the patients are shown in Table 2. A consistent phenotype was present in seven patients carrying homozygous p.R1939Q and four patients who had heterozygous p.R1939Q accompanied by heterozygous truncating or putative splice site mutations. Patient 12, a compound heterozygote of p.R1939Q and a non-truncating mutation, showed a distinct phenoytpe. Patient 13, a homozygote of another non-truncating mutation, presented with temperature-sensitive AN.

Table 2. Genetic and clinical features of patients with congenital or early-onset auditory neuropathy

OTOF genotype[a]	Patient ID	Age, sex	*GJB2* genotype[a]	Degree of hearing loss (age of test)	Phenotype
p.R193Q/p.R1939Q					
	1	3, M	-/-	Profound (1 year 7 months)	NP, flat
	2	2, M	-/-	Profound (2 years 7 months)	NP, flat
	3	3, M	-/-	Profound (3 years 2 months)	NP, flat
	4	4, M	c.235delC/-	Profound (3 years 2 months)	NP, gently sloping
	5	2, F	-/-	profound (2 years 6 months)	NP, gently sloping
	6	2, M	-/-	Severe (2 years 10 months)	NP, flat
	7	2, M	-/-	Severe (1 year 9 months)	NP, flat
p.R1939Q/truncating or putative splice site[b]					
p.R1939Q/c.1946-1965del20	8	9, M	-/-	Unstable (2 years 10 months)	unstable, gently sloping
p.R1939Q/p.Y474X	9	2, M	-/-	Profound (1 year 7 months)	NP, flat
p.R1939Q/p.Y1822X	10	1, F	p.G45E+p.Y136X/-	Profound (2 years 0 month)	NP, flat
p.R1939Q/IVS9+5G>A	11	7, F	-/-	Profound (7 years 6 months)	NP, flat
p.R1939Q/non-truncating[c]					
p.R1939Q/p.X1988RextX30	12	29, F	p.V371/-	Moderate (29 years 1 month)	P, R: steeply sloping L: gently sloping
Non-truncating/non-truncating					
p.G541S/p.G541S	13	26, M	-/-	Mild[d] (25 years 11 months)	NP, flat
Various heterozygotes[e]					
p.R1939Q/-	14	5, F	-/-	Profound (5 years 10 months)	NP, flat
p.D1842N/-	15	2, F	-/-	Moderate (2 years 9 months)	NP, flat
IVS47-2A>G/-	16	6, F	-/-	Profound (5 years 11 months)	NP, flat
No mutations					
	17	4, F	-/-	Severe (4 years 8 months)	NP, gently sloping
	18	7, M	-/-	Profound (7 years 4 months)	NP, gently sloping
	19	6, F	-/-	Severe (5 years 7 months)	NP, R: gently sloping L: flat
	20	8, F	-/-	Profound (8 years 2 months)	NP, gently sloping
	21	3, F	p.235delC/c.176-191del16	Profound (3 years 1 month)	NP, flat
	22	7, F	-/-	Severe (7 years 10 months)	NP, flat
	23	2, M	-/-	Severe (1 year 8 months)	NP, flat

F, female; ID, identification number; M, male; NP, non-progressive; P, progressive; Phenotype (course of hearing loss and audiogram shape).
[a]No mutations.
[b]Truncating or putative splice site mutations.
[c]Non-truncating mutations.
[d]Temperature-sensitive auditory neuropathy.
[e]Mutations in heterozygotes without accompanying pathogenic mutations.

Patient 13 complained of difficulty in understanding conversation, and his hearing deteriorated when he became febrile or was exposed to loud noise according to his self-report. He explained that the deterioration varied from mild to complete loss of communication. Pure-tone audiometry when he was afebrile revealed mild hearing loss with a flat configuration. Among three patients who had only one pathogenic allele of *OTOF*, patient 15 carrying p.D1842N presented with moderate hearing loss, whereas patient 14 carrying p.R1939Q and patient 16 carrying IVS47-2A>G presented with profound hearing loss.

Discussion

The present study demonstrated biallelic *OTOF* mutations in 56.5% (13 of 23) of subjects with congenital or early-onset AN in Japanese population, indicating the most frequent cause associated with this type of AN. So far, biallelic *OTOF* mutations were identified in 22.2% (2 of 9) and 55% (11 of 20) of subjects with AN in American and Spanish studies, respectively (11, 12). In Brazilian population, 27.3% (3 of 11) of subjects with AN had *OTOF* mutations in two alleles (13). Taiwanese and Chinese subjects demonstrated that 18.2% (4 of 22)

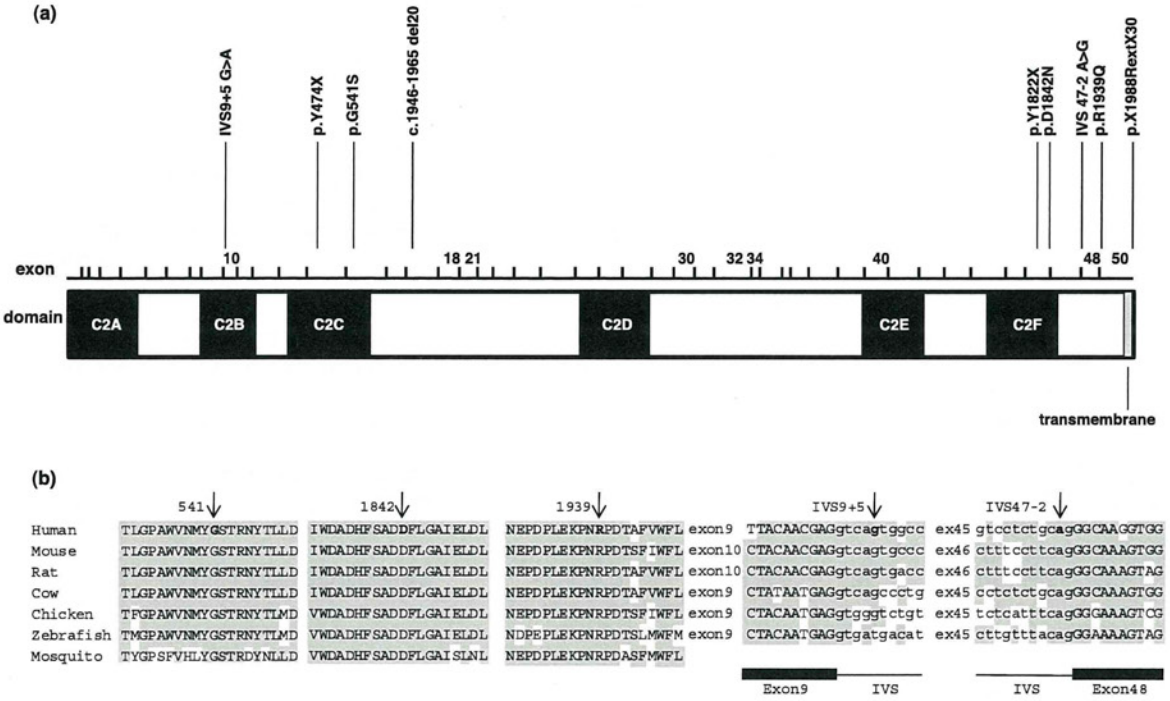

Fig. 2. The location of each mutation in *OTOF* and the evolutionary conservation of the amino acids or nucleotides affected by the missense and splice site mutations. (a) Location of mutations in the *OTOF* coding region of the cochlear isoform. Calcium-binding domains C2A through C2F are shown in black. (b) Multiple alignments of otoferlin orthologs at five non-contiguous regions and splice sites. Arrows indicate affected amino acids or nucleotides. Regions of amino acid and nucleotide sequence identity are shaded. Boundaries between introns and exons are indicated in the bottom. IVS indicates intervening sequence.

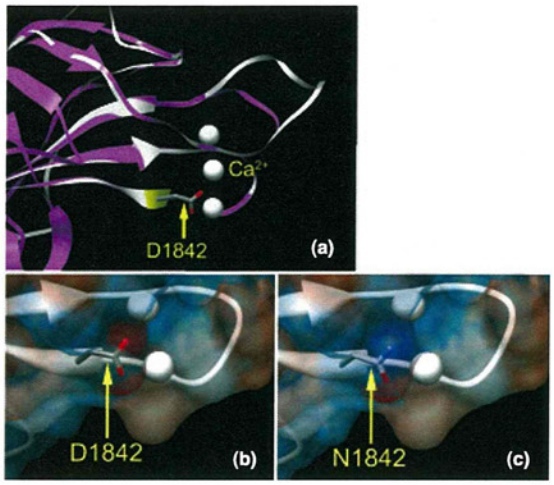

Fig. 3. Predicted three-dimensional protein structures of C2F domain in wild-type otoferlin and D1842N mutant otoferlin. (a) Ribbon model of the otoferlin C2F domain (white) superimposed onto that of the corresponding region of human protein kinase C gamma (hPKCγ, PDBID: 2UZP, chain A) which was selected as an optimal template (29.5% amino acid sequence identity) (magenta). Ca^{2+} is shown as a white sphere. The regions around D1842 of wild-type otoferlin (b) and N1842 of mutant otoferlin (c) are overlaid with their electrostatic surface potentials indicated by red (negative), blue (positive), and white (neutral). The side chains of both D1842 and N1842 are located very close (within 1.0 Å) to calcium ions. D1842N changes the electrostatic surface potential around the side chain from negative to positive in the cellular environment (pH = 7.4), and generate repulsive force on calcium ions.

and 1.4% (1 of 73), respectively, had biallelic *OTOF* mutations (14, 15).

The spectrum of *OTOF* mutations we identified differed significantly from those in other populations. Most reported *OTOF* mutations in the literature have been confined to individual families. An exception is p.Q829X, found in approximately 3% of autosomal recessive non-syndromic sensorineural hearing loss cases in the Spanish population (18). Recently, c.2905-2923delinsCTCCGAGCGCA and p.E1700Q were identified in four Argentinean families and four Taiwanese families, respectively (12, 14). In this study, p.R1939Q was detected in 13 families. Thus, p.R1939Q is now the second-most prevalent *OTOF* mutation reported. This mutation may be more common in Japan, as this mutation is found in only 1 of 10753 choromosomes in the European-American and African-American population by EVS. p.R1939Q was previously reported in one family in the United States, but the origin of the family was not detailed (19). Because no patients carrying p.R1939Q have been reported in Asian population except for the present study or in European population, this prevalent founder mutation appears to be an independent mutational event in Japanese.

Pathogenic *OTOF* mutations have been associated with stable, severe-to-profound sensorineural hearing loss with a few exceptions: c.2093+1G>T and p.P1987R were associated with stable, moderate-to-severe hearing loss (11, 19), p.E1700Q was associated with progressive, moderate-to-profound hearing

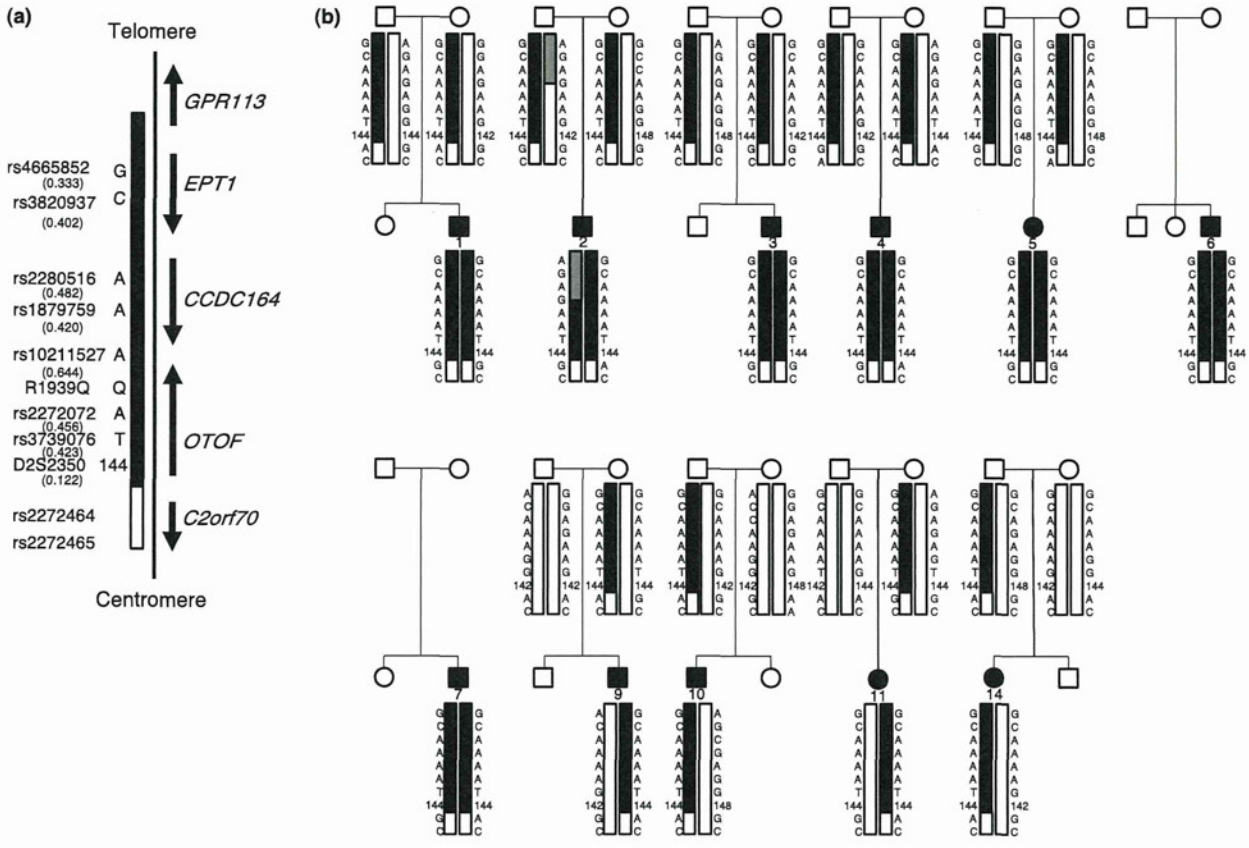

Fig. 4. Results of haplotype analysis of patients who had p.R1939Q alleles and their parents. (a) A part of tested single nucleotide polymorphisms (SNPs) and a microsatellite marker in relation to the genetic map around *OTOF* (chromosome 2p23.1). The region corresponding to the haplotype associated with the p.R1939Q mutation is indicated by black. Allele frequency of each SNP and a microsatellite marker is shown in a parenthesis. (b) Haplotypes of 11 auditory neuropathy (AN) patients with hearing loss who had p.R1939Q and their parents. The haplotype is indicated beside the vertical bars. The number under the symbol is the patient identification number in Table 2. A recombination point is indicated by grey in patient 2.

loss (14), and several mutations were associated with temperature-sensitive AN (11, 13, 15, 20). p.R1939Q homozygotes had a consistent phenotype of congenital or early-onset, stable, and severe-to-profound hearing loss with a flat or gently sloping audiogram. The same phenotype has also been reported in a family in United States, which included compound heterozygotes having p.R1939Q and a truncating mutation (19). Patients that were compound heterozygotes of p.R1939Q and truncating mutations or a putative splice site mutation also exhibited the similar phenotype in the present study. Thus, p.R1939Q variants are likely to cause severe impairment of otoferlin function. In contrast, a subject that was a compound heterozygote of p.R1939Q and a non-truncating mutation presented with a distinct phenotype of congenital or early-onset, progressive, moderate hearing loss with a steeply sloping or gently sloping audiogram. A homozygote of another non-truncating mutation also showed a distinct phenotype of temperature-sensitive AN. One of three patients who had only one allele of non-truncating mutation other than p.R1939Q presented with moderate hearing loss, whereas the other two subjects who had only one allele of p.R1939Q or a putative splice site mutation presented with profound hearing loss. These genotype–phenotype correlations of *OTOF* were similar to those of *GJB2*, i.e., more severe hearing loss was observed in subjects homozygous for truncating mutations than in subjects homozygous for non-truncating mutations, and more severe hearing loss was observed in subjects homozygous for a frameshift mutation (35delG) than in subjects compound heterozygous for the 35delG and other mutations (26, 27).

A patient with temperature-sensitive AN with a specific *OTOF* mutation was found in the present study. So far, temperature-sensitive AN has been observed in two siblings with heterozygous p.I515T without an accompanying pathogenic allele (11), three siblings with homozygous p.E1804del (20), a compound heterozygote with c.2975-2978delAG and p.R1607W (15), and a compound heterozygote with p.G614E and p.R1080P (13). The patient in this study had biallelic mutations affecting residues specific to the long isoform. Previously, two subjects showed biallelic mutations affecting this region, but they were not tested for OAE (16, 17). Thus, the present patient is the first case with biallelic mutations in this region, which indicates that mutations in the *OTOF* long isoform alone are able to cause AN.

Supporting Information

The following Supporting information is available for this article:
Table S1. Primer sequences for *OTOF*.
Table S2. Primer sequences for *PJVK*.

Additional Supporting information may be found in the online version of this article.

Please note: Wiley-Blackwell Publishing is not responsible for the content or functionality of any supplementary materials supplied by the authors. Any queries (other than missing material) should be directed to the corresponding author for the article.

Acknowledgements

We thank the families that participated in this study. We also thank Dr Yasuhide Okamoto (Inagi Municipal Hospital) and Dr Seiichi Shinden (Saiseikai Utsunomiya Hospital) for their invaluable contribution. This study was supported by a research grant of Comprehensive Research on Disability Health and Welfare from the Ministry of Health, Labor, and Welfare of Japan and a Grant-in-Aid for Clinical Research from the National Hospital Organization.

References

1. Starr A, Picton TW, Sininger Y, Hood LJ, Berlin CI. Auditory neuropathy. Brain 1996: 119: 741–753.
2. Kaga K, Nakamura M, Shinogami M, Tsuzuku T, Yamada K, Shindo M. Auditory nerve disease of both ears revealed by auditory brainstem responses, electrocochleography and otoacoustic emissions. Scand Audiol 1996: 25: 233–238.
3. Rance G, Beer DE, Cone-Wesson B et al. Clinical findings for a group of infants and young children with auditory neuropathy. Ear Hear 1999: 20: 238–252.
4. Foerst A, Beutner D, Lang-Roth R, Huttenbrink KB, von Wedel H, Walger M. Prevalence of auditory neuropathy/synaptopathy in a population of children with profound hearing loss. Int J Pediatr Otorhinolaryngol 2006: 70: 1415–1422.
5. Raveh E, Buller N, Badrana O, Attias J. Auditory neuropathy. clinical characteristics and therapeutic approach. Am J Otolaryngol 2007: 28: 302–308.
6. Yasunaga S, Grati M, Cohen-Salmon M et al. A mutation in OTOF, encoding otoferlin, a FER-1-like protein, causes DFNB9, a nonsyndromic form of deafness. Nat Genet 1999: 21: 363–369.
7. Delmaghani S, del Castillo FJ, Michel V et al. Mutations in the gene encoding pejvakin, a newly identified protein of the afferent auditory pathway, cause DFNB59 auditory neuropathy. Nat Genet 2006: 38: 770–778.
8. Schoen CJ, Emery SB, Thorne MC et al. Increased activity of Diaphanous homolog 3 (DIAPH3)/diaphanous causes hearing defects in humans with auditory neuropathy and in Drosophila. Proc Natl Acad Sci USA 2010: 107: 13396–13401.
9. Wang QJ, Li QZ, Rao SQ et al. AUNX1, a novel locus responsible for X linked recessive auditory and peripheral neuropathy, maps to Xq23-27.3. J Med Genet 2006: 43: e33.
10. Yasunaga S, Grati M, Chardenoux S et al. OTOF encodes multiple long and short isoforms: genetic evidence that the long ones underlie recessive deafness DFNB9. Am J Hum Genet 2000: 67: 591–600.
11. Varga R, Avenarius MR, Kelley PM et al. OTOF mutations revealed by genetic analysis of hearing loss families including a potential temperature sensitive auditory neuropathy allele. J Med Genet 2006: 43: 576–581.
12. Rodríguez-Ballesteros M, Reynoso R, Olarte M et al. A multicenter study on the prevalence and spectrum of mutations in the otoferlin gene (OTOF) in subjects with nonsyndromic hearing impairment and auditory neuropathy. Hum Mutat 2008: 29: 823–831.
13. Romanos J, Kimura L, Fávero ML et al. Novel OTOF mutations in Brazilian patients with auditory neuropathy. J Hum Genet 2009: 54: 382–385.
14. Chiu YH, Wu CC, Lu YC et al. Mutations in the OTOF gene in Taiwanese patients with auditory neuropathy. Audiol Neurootol 2010: 15: 364–374.
15. Wang DY, Wang YC, Weil D et al. Screening mutations of OTOF gene in Chinese patients with auditory neuropathy, including a familial case of temperature-sensitive auditory neuropathy. BMC Med Genet 2010: 26: 79.
16. Choi BY, Ahmed ZM, Riazuddin S et al. Identities and frequencies of mutations of the otoferlin gene (OTOF) causing DFNB9 deafness in Pakistan. Clin Genet 2009: 75: 237–243.
17. Mirghomizadeh F, Pfister M, Apaydin F et al. Substitutions in the conserved C2C domain of otoferlin cause DFNB9, a form of nonsyndromic autosomal recessive deafness. Neurobiol Dis 2002: 10: 157–164.
18. Rodríguez-Ballesteros M, del Castillo FJ, Martín Y et al. Auditory neuropathy in patients carrying mutations in the otoferlin gene (OTOF). Hum Mutat 2003: 22: 451–456.
19. Varga R, Kelley PM, Keats BJ et al. Non-syndromic recessive auditory neuropathy is the result of mutations in the otoferlin (OTOF) gene. J Med Genet 2003: 40: 45–50.
20. Marlin S, Feldmann D, Nguyen Y et al. Temperature-sensitive auditory neuropathy associated with an otoferlin mutation: Deafening fever!. Biochem Biophys Res Commun 2010: 394: 737–742.
21. Matsunaga T, Hirota E, Bito S, Niimi S, Usami S. Clinical course of hearing and language development in GJB2 and non-GJB2 deafness following habilitation with hearing aids. Audiol Neurootol 2006: 11: 59–68.
22. Usami S, Abe S, Akita J et al. Prevalence of mitochondrial gene mutations among hearing impaired patients. J Med Genet 2000: 37: 38–40.
23. Kiefer F, Arnold K, Künzli M, Bordoli L, Schwede T. The SWISS-MODEL Repository and associated resources. Nucleic Acid Res 2009: 37: 387–392.
24. Hilleren P, Parker R. Mechanisms of mRNA surveillance in eukaryotes. Annu Rev Genet 1999: 33: 229–260.
25. Cheng X, Li L, Brashears S et al. Connexin 26 variants and auditory neuropathy/dys-synchrony among children in schools for the deaf. Am J Med Genet A 2005: 139: 13–18.
26. Cryns K, Orzan E, Murgia A et al. Genotype-phenotypecorrelation for GJB2 (connexin 26) deafness. J Med Genet 2004: 41: 147–154.
27. Snoeckx RL, Huygen PL, Feldmann D et al. GJB2 mutations and degree of hearing loss: a multicenter study. Am J Hum Genet 2005: 77: 945–957.

Gene 501 (2012) 193–197

Contents lists available at SciVerse ScienceDirect

Gene

journal homepage: www.elsevier.com/locate/gene

Comorbidity of *GJB2* and *WFS1* mutations in one family

Shujiro B. Minami [a,b,*], Sawako Masuda [c], Satoko Usui [c], Hideki Mutai [b], Tatsuo Matsunaga [a,b]

[a] NHO Tokyo Medical Center, Department of Otolaryngology, Japan
[b] NHO Tokyo Medical Center, National Institute of Sensory Organs, Laboratory of Auditory Disorders, Japan
[c] NHO Mie Hospital, Department of Otolaryngology, Japan

ARTICLE INFO

Article history:
Accepted 22 March 2012
Available online 31 March 2012

Keywords:
Connexin 26
Hereditary hearing loss
Wolframin
DFNB1
DFNA6/14

ABSTRACT

It is rarely reported that two distinct genetic mutations affecting hearing have been found in one family. We report on a family exhibiting comorbid mutation of *GJB2* and *WFS1*. A four-generation Japanese family with autosomal dominant sensorineural hearing loss was studied. In 7 of the 24 family members, audiometric evaluations and genetic analysis were performed. We detected A-to-C nucleotide transversion (c.2576G>C) in exon 8 of *WFS1* that was predicted to result in an arginine-to-proline substitution at codon 859 (R859P), G-to-A transition (c.109G>A) in exon 2 of *GJB2* that was predicted to result in a valine-to-isoleucine substitution at codon 37 (V37I), and C-to-T transition (c.427C>T) in exon 2 of *GJB2* that was predicted to result in an arginine-to-tryptophan substitution at codon 143 (R143W). Two individuals who had heterozygosity of *GJB2* mutations and heterozygosity of *WFS1* mutations showed low-frequency hearing loss. One individual who had homozygosity of *GJB2* mutation without *WFS1* mutation had moderate, gradual high tone hearing loss. On the other hand, a moderate flat loss configuration was seen in one individual who had compound heterozygosity of *GJB2* and heterozygosity of *WFS1* mutations. Our results indicate that the individual who has both *GJB2* and *WFS1* mutations can show *GJB2* phenotype.

1. Introduction

More than half the incidence of congenital hearing loss is due to hereditary factors (Smith et al., 2005). Owing to recent advances in molecular genetics, more than 400 genetic syndromes have been associated with hearing loss and more than 140 genetic loci associated with nonsyndromic hearing loss have been mapped, with more than 60 genes identified to date (Van Camp G, Smith RJH. Hereditary Hearing Loss Homepage, last updated 2011 June 17. Available at: http://hereditaryhearingloss.org). Hereditary hearing loss can be inherited as an autosomal dominant, autosomal recessive, X-linked or mitochondrial (maternally inherited) condition. It is rarely reported that two distinct genetic mutations linked to hearing loss have been found in one family. Now we report on a family exhibiting comorbid mutations of *GJB2* and *WFS1*.

Mutations in the *GJB2* gene encoding connexin 26 are the most common cause of nonsyndromic autosomal recessive sensorineural hearing loss (DFNB1) in many populations (Estivill et al., 1998; Matsunaga et al., 2006; Morell et al., 1998). To date, more than 150 mutations, polymorphisms, and unclassified variants have been described in the *GJB2* gene (http://davinci.crg.es/deafness). The mutation spectrum and prevalence of mutations vary significantly across different ethnic groups (Dai et al., 2009; Estivill et al., 1998; Morell et al., 1998; Ohtsuka et al., 2003). SNHL-causing allele variants of *GJB2* alter the function of the encoded protein, connexin 26, in the inner ear. Connexin 26 aggregates in groups of six around a central 2–3 nm pore to form a doughnut-shaped structure called a connexon (Maeda et al., 2009). The connexons from contiguous cells covalently bond to form intercellular channels. Aggregations of connexons are called plaques and are the constituents of gap junctions. The gap junction system might be involved in potassium circulation, allowing ions that enter hair cells during mechanosensory transduction to be recycled to the stria vascularis (Zdebik et al., 2009).

The *WFS1* gene maps to chromosome 4p16, and has a transcript of 3640 nucleotides of which 2673 bp are coding. *WFS1* consists of 8 exons, of which the first exon is non-coding. The largest exon is exon 8, where the coding part is 1812 bp long. Numerous sequence variants/polymorphisms, mainly in exon 8 of *WFS1*, have been reported (Cryns et al., 2003a). *WFS1* extends over 33.4 kb of genomic DNA. The gene transcribes an mRNA of 3.6 kb that encodes wolframin, an 890-amino-acid protein with a predicted molecular mass of 100 kDa (Inoue et al., 1998). Its function within the inner ear is currently unknown, but its localization in the endoplasmic reticulum (ER) suggests a possible role for wolframin in ion homeostasis maintained by the canalicular reticulum, a specialized form of ER (Cryns et al., 2003b). Mutations in *WFS1* underlie autosomal recessive Wolfram syndrome (MIM# 222300) (Strom et al., 1998) and autosomal dominant low frequency sensorineural

Abbreviations: ABRs, Auditory Brainstem Responses; ASSR, Auditory Steady-State Response.

* Corresponding author at: 2-5-1 Higashigaoka Meguro-ku, Tokyo 152-8902, Japan. Tel.: +81 3 3411 0111; fax: +81 3 3412 9811.
E-mail address: shujirominami@me.com (S.B. Minami).

0378-1119/$ – see front matter © 2012 Elsevier B.V. All rights reserved.
doi:10.1016/j.gene.2012.03.060

hearing impairment (LFSNHI) DFNA6/14 (MIM# 600965) (Bespalova et al., 2001; Young et al., 2001). Hearing impairment in Wolfram syndrome is progressive and mainly affects the high frequencies (Higashi, 1991). In contrast, hearing impairment associated with DFNA6/14 affects only the low frequencies and it shows little or no progression (Bom et al., 2002; Brodwolf et al., 2001; Kunst et al., 1999; Lesperance et al., 2003; Pennings et al., 2003). This is the first report of a family with comorbid hereditary hearing loss of DFNB1 and DFNA6/14.

2. Materials and methods

2.1. Family report

All the procedures were approved by the Ethics Review Committee of National Tokyo Medical Center and were carried out only after a written informed consent had been obtained from each individual or parents of the children.

A four-generation Japanese family with autosomal dominant sensorineural hearing loss was studied (Fig. 1). The family does not have a history of diabetes mellitus, dysopia, nor psychiatric disorders, which are the characteristic symptoms of Wolfram syndrome. In 7 of the 23 family members, audiometric evaluations and a genetic analysis were performed. Information regarding hearing loss in the other 16 family members was obtained through interviews with the 7 family members. Pure tone audiometry was carried out in all participants, with the exception of the proband, who was 1 year of age. Hearing loss in the proband was assessed via Auditory Brainstem Responses (ABRs) and Auditory Steady-State Response (ASSR). During the recording sessions for evoked audiometry (ABR and ASSR), the patient was in a state of induced sleep. He was sedated with triclofos sodium (80 mg/kg, administered orally). ABR and ASSR studies were obtained using the AUDERA device (Grason-Stadler).

2.2. Genetic analysis

Based on the age and audiometric configurations of the family members, we screened for the presence of *GJB2* and *WFS1* mutations (Matsunaga, 2009). The entire coding regions of*GJB2* were amplified using the primer pair Cx48U/Cx1040L (Matsunaga et al., 2006). Coding exons 2–7 of WFS1 were amplified using primers and the PCR protocol previously described (Strom et al., 1998). For the coding sequence in exon 8 of *WFS1*, three primer pairs were designed, yielding overlapping products of around 700 base pairs. The primer pairs are as follows: 5′-AGGCGTGAGATGGGAGCAGT-3′ and 5′-AGGCGTGAGATGGGAGCAGT-3′, 5′-TGGTGTGCTTCATGTGGTG-3′ and 5′-TGGCATGCCCACGGTAATCT-3′, 5′-ATCGTGCTGTTCTGCTGGTTC-3′ and 5′-ACACATGGTCGCAAGGTCTC-3′. Polymerase chain reaction products were sequenced and analyzed with an ABI sequencer 377XL (PerkinElmer).

3. Results

Individual IV-3 is the proband, a 1-year-old boy. He was born a low-birth-weight baby (1861 g) after a gestation of 30 weeks and 6 days, and admitted to a neonatal intensive care unit. He underwent the ABR test at 8-months-old and the wave V in responses to click noises of 40 dB on both sides was confirmed (Figs. 2A,B). ASSR test at one year of age showed a low-frequency hearing loss (Figs. 2C,D). In the proband, we detected a heterozygous A-to-C nucleotide transversion (c.2576G>C) in exon 8 of *WFS1* that was predicted to result in an arginine-to-proline substitution at codon 859 (R859P), which was reported as a pathological mutation. The proband also had a heterozygous G-to-A transition (c.109G>A) in exon2 of *GJB2* that was predicted to result in avaline-to-isoleucine substitution at codon 37 (V37I). Individual IV-2 had low frequency sensorineural hearing loss with pure tone audiometry at 4 years of age as well (Fig. 3A). Sequencing of *GJB2* and *WFS1* revealed a heterozygous C-to-T transition (c.427C>T) in exon2 of *GJB2* that was predicted to result

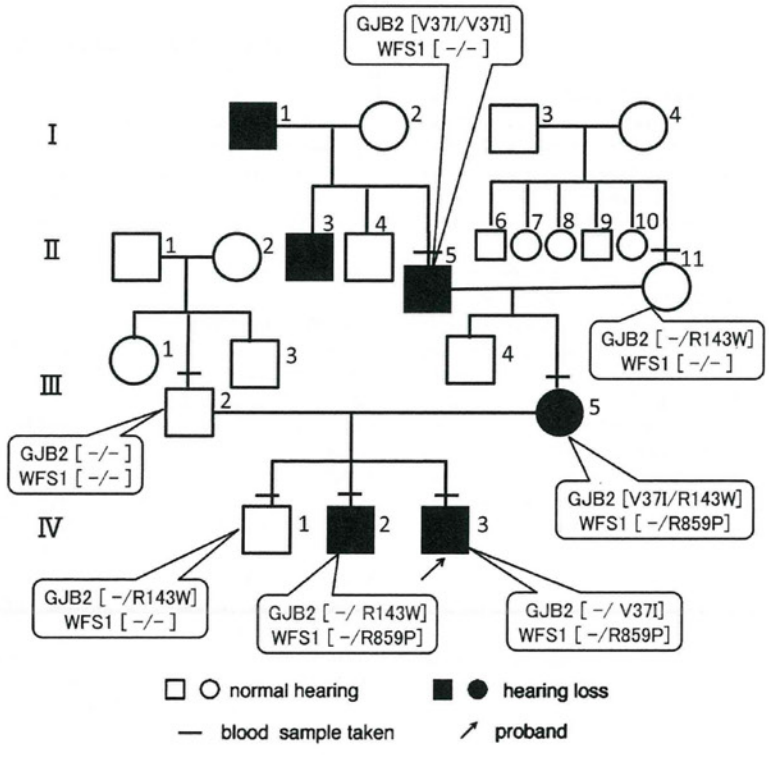

Fig. 1. Pedigree of the DFNB1/DFNA6/14 family.